J. Electrochem. Sci. Eng. **16** (2026) 3341; https://doi.org/10.5599/jese.3341

Open Access : : ISSN 1847-9286
https://pub.iapchem.org/ojs/index.php/JESE

Original scientific paper

Graphene oxide/NiO nanocomposite-modified carbon paste electrode for the simultaneous detection of carmoisine and tartrazine as two azo dyes in food samples

Fares A. Yasseen[1,✉], Ali Obaid Imarah[2], Rasha Faris Hadi[3,4] and Huda Hadi Nameh[4]

[1]*Department of Physics, Faculty of Science, University of Kufa, Al-Najaf, Iraq*
[2]*Chemical Engineering Department, College of Engineering, University of Babylon, Iraq*
[3]*Department of Biomedical Engineering, College of Engineering, University of Babylon, Iraq*
[4]*Faculty of Education, Department of Chemistry, University of Hilla, Babylon, 51001, Iraq*

Corresponding Author: ✉fares.alkufy@uokufa.edu.iq

Received: February 8, 2026; Accepted: April 20, 2026; Published: April 29, 2026

Abstract

A carbon paste electrode (CPE) was modified with a graphene oxide (GO)/NiO nanocomposite (GO/NiO/CPE) and used as the working electrode for the voltammetric analysis of carmoisine. In the oxidation of carmoisine, the GO/NiO/CPE showed increased electrocatalytic activity. With a detection limit of 0.1 μM under ideal conditions, the oxidation peak currents of carmoisine were linearly proportional to its concentration over the range 0.3 to 500.0 μM. Additionally, the GO/NiO/CPE showed good efficacy in detecting carmoisine even in the presence of tartrazine, suggesting that both chemicals might be determined simultaneously. The GO/NiO/CPE was appropriate for the simultaneous detection of carmoisine and tartrazine using differential pulse voltammetry because the oxidation peak potentials of the two azo dyes were adequately separated by 420 mV.

Keywords

Food colorants, electrochemical sensing; hybrid composite; voltammetry, powdered juice

Introduction

Food colorants are chemicals that improve the visual appearance of food and beverage products when applied. The food processing industry applies both natural and artificial edible colorants to its operations [1]. Food colorants enhance visual appeal and help restore food products to their original appearance, which can be altered by processing, storage, packing, and distribution [2]. Synthetic colorants, which include azo dyes, have become common in the food industry because these substances create appealing colour effects while simultaneously providing excellent water solubility,

low production costs, low microbial contamination, and high stability against light, oxygen and pH changes [1].

Synthetic dyes now have extensive applications across multiple industries, which include plastic and textile, leather, detergent and cosmetic manufacturing sectors. The organoleptic properties of food products are enhanced by their use [3,4]. Azo dyes, the most significant group of synthetic dyes, first appeared following Griess's discovery in 1865 [5,6]. Azo dyes demonstrate high water solubility because their chemical structure includes an azo chromophore together with aromatic groups. This dye contains an N=N double bond, an active functional group. Azo dyes can exist as mono-azo dyes, diazo dyes or poly-azo dyes based on their total count of azo functional groups [7]. Most commercial dyes in this group are mono-azo dyes [5].

Azo dyes are included in half of all commercially available dyestuffs [8]. The most widespread synthetic dye family is azo dyes, as organic materials reach their highest production and usage levels worldwide [8]. Many textile companies use azo dyes because these dyes possess special physical and chemical characteristics that enable their application in the pharmaceutical, cosmetic and leather sectors [8]. The substances function as industrial materials while they serve as food colorants, drug delivery systems and biomedical research tools [8]. The azo groups, which form chromophores in azo dyes, lead to the development of hazardous aromatic amines exhibiting biological toxicity [8]. Human health risks arise from both azo dyes and their breakdown products. People should avoid consuming these substances beyond safe limits because excessive intake poses risks for food safety and human health [9]. A few azo dyes cause asthma together with touch hypersensitivity as documented adverse effects. Azo dyes cause food prejudice together with hypersensitivity and hyperactivity disorders [9]. The European Union Regulation (EC) 1907/2006 prohibits the use of certain azo dyes because these substances pose serious hazards to human health and environmental safety.

The analysis of key chemical substances requires highly accurate detection methods for precise control. Carmoisine, a synthetic red dye containing an azo linkage in its chemical structure, imparts a typical red-to-maroon hue to food and drinks [10].

The use of carmoisine as a colouring agent for jams and preserves dates back to ancient times, but most industrialized countries later banned its use because of its beta-naphthylamine content, which scientists recognized as a carcinogen [10]. Many azo dyes undergo reductive cleavage of their azo groups, which produces an aromatic amine that exhibits carcinogenic properties. The dye causes nettle rash, water retention, asthma, and medicine intolerance in numerous individuals [11].

Dye consumption at high levels produces coma and convulsions and somnolence, together with death, while aggravating behavioural issues in children who experience hyperactivity, tantrums and sleeplessness. The food industry requires strict monitoring of carmoisine because rapid, sensitive detection methods for carmoisine are vital for food security and human well-being [12].

The food additive tartrazine, which belongs to the azo synthetic food colorant group, has become a common ingredient in food products, beverages, and pharmaceuticals. Monitoring tartrazine levels in dietary intake is essential due to this requirement [13]. Excessive tartrazine consumption leads to multiple health problems, which include food intolerance, hyperactivity, asthma, allergies, cutaneous toxicity, acute oral toxicity and cancer [14] development. The evaluation of tartrazine content in food products is necessary to enhance food safety standards. The analysis of carmoisine and tartrazine can be performed through multiple methods, which include high-performance liquid chromatography, capillary electrophoresis, spectrophotometry and colorimetric analysis [15]. The other techniques present operational challenges because they require extended analysis periods, their testing costs remain high, particular materials must undergo pretreatment, and their

equipment requires complicated setups. Electrochemical methods provide testing solutions that enable fast and affordable operations while delivering highly sensitive test results [16]. The electrochemical analysis process uses carbon-based electrodes because these materials offer chemical inertness combined with low background current, low-cost operation and broad potential range and precise sensing capabilities [17]. Researchers have recently developed multiple sensors that detect bioactive substances through electrochemical methods [18].

Carbon electrodes serve as common components for electroanalysis because they combine multiple features, which include low background current, wide potential range, chemical inertness, cost efficiency and ability to work in multiple sensing and detection fields [19]. The carbon electrode category includes carbon paste electrodes CPE which hold special importance. CPEs provide multiple benefits that surpass all other carbon electrodes because they feature a porous structure, and they show extremely low background current, which is below the level of graphite electrodes, and offer inexpensive materials and allow for multiple ingredient combinations during paste creation, and provide fast and simple methods to create new surfaces that maintain reproducible qualities [20]. Over the years, various CPEs with different modifiers have been developed and used to analyse different analytes [21].

The type of materials that make up the detection platform is crucial for obtaining a high-quality, reliable electrochemical sensor. The combination of electrochemical sensor technology with nanomaterials will yield operational benefits, which scientists will investigate by implementing these nanomaterials as electrochemical labels and signal-enhancement devices for new transduction systems [22]. Sensors that use nanostructured materials outperform bulk-material-based electrodes because they provide larger electrode surface areas and better mass transport and rapid electron-transfer capabilities [22]. Nanomaterials enable researchers to develop cost-effective electrode production techniques that require less material and produce less waste through their distinctive properties [23].

Recent research efforts have led to the development of various nanostructured materials that improve the performance of electrochemical sensors. Metal oxide nanomaterials-based electrochemical sensors have become popular because their electrochemical performance is driven by their high surface area and low production costs [24,25].

The electrochemical research field has improved its sensitivity and detection limit using nickel oxide nanoparticles (NiO-NPs), which function as p-type semiconductors with exceptional biological compatibility, broad surface area, stable performance, high conductivity and electrocatalytic properties [26].

Researchers have extensively studied graphene in recent years because this material consists of a single layer of sp2-hybridized carbon atoms that form a dense honeycomb two-dimensional lattice, have a large surface area, and exhibit various mechanical and electrical characteristics, as well as numerous applications that researchers have tested using graphene-based materials [27].

The oxygenated hydrophilic layered carbon material, graphene oxide (GO), which people derive from graphene, has attracted scientists because of its light weight and high surface area, its availability as bulk material, its inexpensive production method, and its ability to disperse in water and its capacity to undergo chemical reactions for multiple practical uses [28]. The benefits of these materials enable scientists to use graphene and NiO for the electrocatalytic oxidation of various analytes, as reported by their findings [29]. The results show that the NiO-graphene oxide nanocomposite exhibits superior electrocatalytic performance compared to its individual components. The electrochemical response of carmoisine is improved by the addition of NiO particles to graphene oxide [29].

The current work aimed to develop an advanced electrochemical sensor capable of detecting tartrazine and carmoisine simultaneously. The modified electrode showed electrochemical

behaviour of carmoisine through CPE modification, while cyclic voltammetry (CV), linear sweep voltammetry (LSV), differential pulse voltammetry (DPV) and chronoamperometry (CHA) tests demonstrated its electrochemical performance. The oxidation signal of carmoisine on GO/NiO/CPE was compared with that on an unmodified electrode. The manufactured electrode measured carmoisine and tartrazine simultaneously. The successful results from GO/NiO/CPE testing established it as a certified sensor for tartrazine and carmoisine detection.

Experimental

Chemicals and reagents

Merck chemicals (Germany) provided carmoisine, tartrazine, paraffin oil, graphite powder, sodium dihydrogen orthophosphate monohydrate ($NaH_2PO_4 \cdot H_2O$, 98.0 %), and dipotassium hydrogen orthophosphate (K_2HPO_4, 98 %). All electrochemical investigations used a freshly made 0.1 M phosphate-buffered saline (PBS) solution made from the phosphate salts mentioned above as the supporting electrolyte. Double-distilled water with a resistivity of 15 MΩ cm was used for all solution formulations during the studies.

Synthesis of graphene oxide/NiO nanocomposite

To ensure homogeneity of the suspension, 0.01 g of GO was sonicated for 1 h in 20 mL of deionized water with 1.2 mmol of $Ni(NO_3)_2 \cdot 6H_2O$ and 12 mmol of urea. The mixture was stirred for 20 minutes, then placed in an autoclave and heated to 100 °C for 12 hours. Following the reaction, the precipitates were recovered by centrifugation and repeatedly cleaned with ethanol. The material was dried for 12 hours at 65 °C. The GO/NiO nanocomposite was then produced by calcining the prepared product in air at 400 °C for 4 h. Figure 1 shows the GO/NiO nanocomposite's SEM picture using the TESCAN MIRA3 scanning electron microscope (Czech Republic).

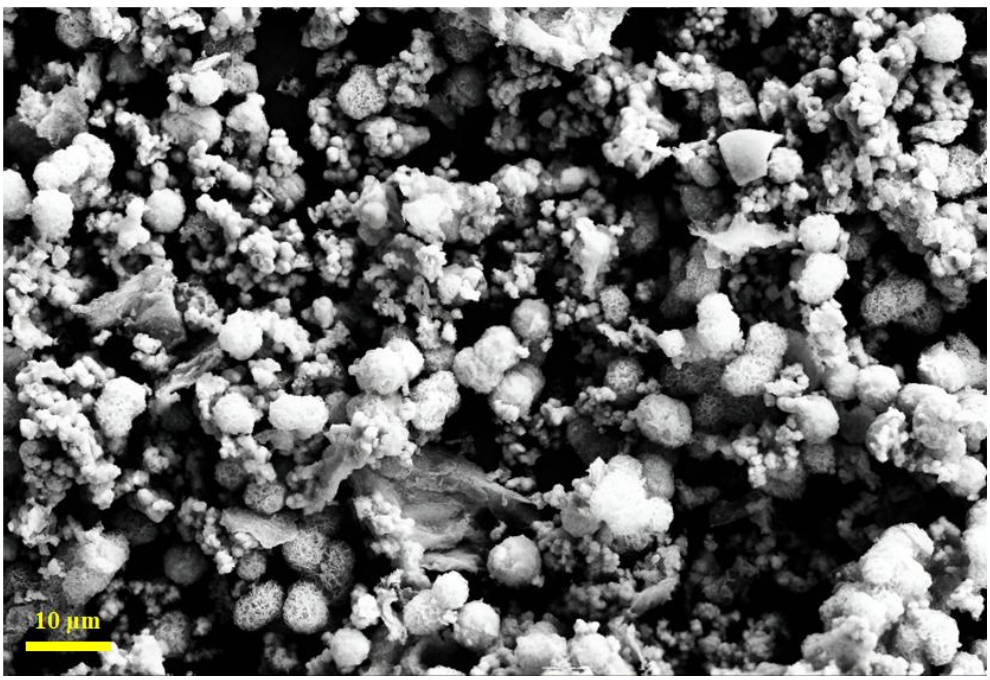

***Figure 1**. SEM image of GO/NiO nanocomposite*

Preparation of graphene oxide/NiO/carbon paste electrode sensor

For preparing GO/NiO/CPE, 0.1 g of GO/NiO nanocomposite was combined with 0.9 g of graphite powder and mineral oil to create a paste that maintained its properties throughout the duration of

the experiments. A mortar and pestle were used to mix the ingredients for ten minutes to produce a consistent material. Then the paste was applied to the electrode's sensing area for testing purposes.

Preparation of real samples

The powdered juice sample was prepared by dissolving 5 g of the powder in 50 mL of deionized water (50 ˚C) and allowing the mixture to cool to room temperature. Next, 10 mL of 0.1 M phosphate buffer (pH 7.0) was added to dilute the solution. The diluted solution was then filtered using a membrane filter (0.45 µm).

Electrochemical methods

A Metrohm microAutolab electrochemical workstation was used for all electrochemical studies. Three electrodes were used in the electrochemical characterization of azo dyes: the working electrode was GO/NiO/CPE (geometric area of 0.0314 cm^2), the counter electrode was a Pt wire, and the reference electrode was Ag/AgCl (3.0 M KCl). cyclic voltammetry (CV). The GO/NiO/CPE were selected for carmoisine detection using differential pulse voltammetry because of their better electrochemical performance. pH (optimum value of 7.0), applied potential (initial potential of 270 mV and end potential of 960 mV for calibration curve), step potential (optimum value of 0.01 V) and pulse amplitude (optimum value of 0.025 V) were among the critical parameters that were tuned. To ascertain the limit of detection (LOD), a calibration curve was created. To ensure consistent and reliable performance, the sensor's repeatability, reproducibility, and stability were also carefully assessed.

Results and discussion

The electrochemical performance of graphene oxide/NiO/carbon paste electrode for carmoisine

Because protons are involved in the oxidation process, the pH of the PBS solution significantly affects the electroanalysis of carmoisine. Therefore, using DPV, the electrochemical behaviour of carmoisine was investigated on the surface of GO/NiO/CPE in PBS (0.1 M, pH 2.0 to 9.0). According to DPV data, the highest current value was obtained for carmoisine oxidation at pH 7.0. Therefore, pH 7.0 was used for additional electrochemical experiments.

Figure 2 shows the CVs obtained for carmoisine (100.0 µM) on unmodified CPE and GO/NiO/CPE in phosphate buffer at pH 7.0.

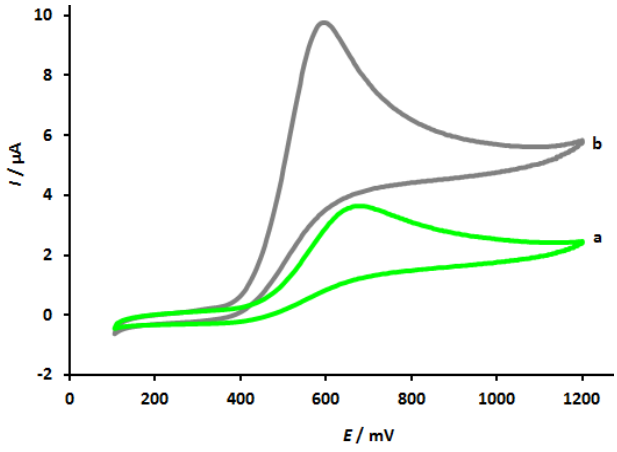

***Figure 2**. CVs (50 mV s^{-1}) obtained on (a) unmodified CPE and (b) GO/NiO/CPE in phosphate buffer (0.1 M, pH 7.0) in the presence of 100.0 µM carmoisine*

The unmodified CPE, carmoisine, exhibited an electrochemical reaction with an oxidation peak current height of I_{pa} = 3.6 µA. On the Ni-GO/NiO/CPE, the I_{pa} of carmoisine increased to 9.7 µA.

Additionally, the peak potential of oxidation (E_{pa}) decreased from 680 mV on the unmodified CPE surface to 600 mV on the GO/NiO/CPE surface. These findings therefore demonstrate the appropriate catalytic effect of GO/NiO/CPE for the carmoisine oxidation process.

Effect of scan rate

Determining how the scan rates affected the carmoisine oxidation peak current was the next step (Figure 3). Based on the observed CVs, the oxidation peak current of carmoisine increased with increasing scan rate. Plots of the current peak height (I_p) against the square root of the scan rate ($\nu^{1/2}$) are shown in Figure 3 (inset). Based on the linearity of the resultant plot, it was concluded that the reaction of carmoisine on the GO/NiO/CPE is under diffusion control.

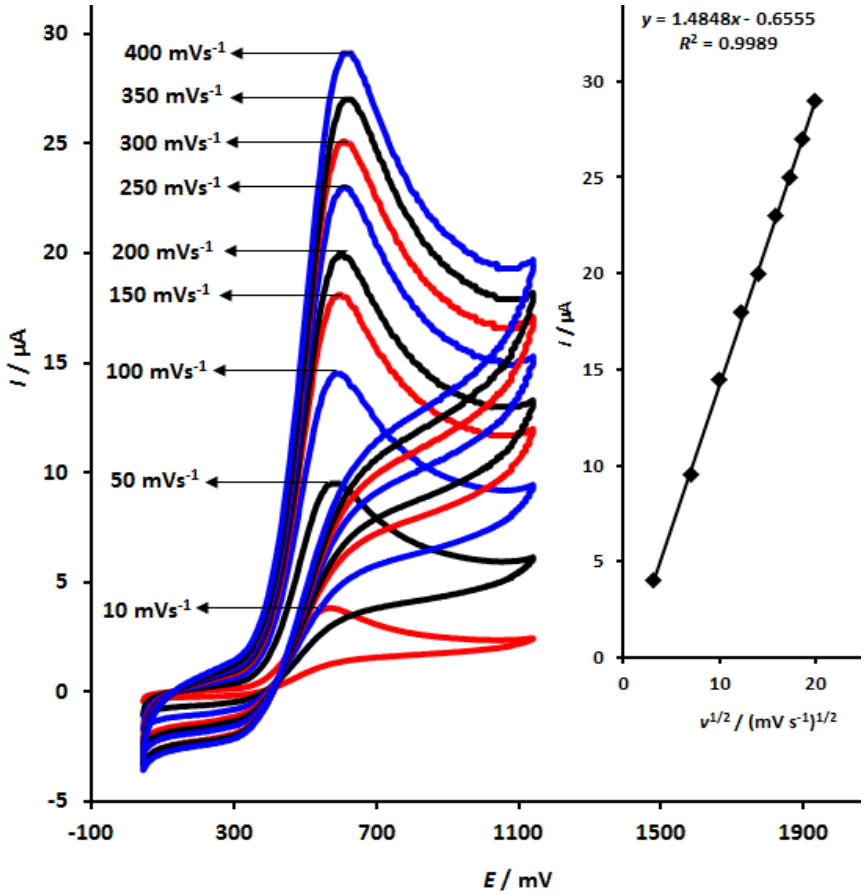

***Figure 3**. CVs of GO/NiO/CPE at various scan rates (10 to 400 mV s^{-1}) in phosphate buffer (0.1 M, pH 7.0) containing 100.0 µM carmoisine. Inset: changes in the I_p as a function of $\nu^{1/2}$*

Next, data from the ascent of the *I-E* curve captured at 10 mV s^{-1} were used to create a Tafel plot (Figure 4). The Tafel region would be affected by the kinetics of electron transfer between carmoisine and the GO/NiO/CPE. The anodic transfer coefficient (α) may be calculated from the slope of the Tafel plot using Equation (1).

$$\eta = \frac{2.303\ RT}{(1\text{-}\alpha)nF}\log I + \text{constant} \qquad (1)$$

In Equation (1) η / V is overpotential, R is the gas constant (8.314 J mol^{-1} K^{-1}), T / K is absolute temperature, F is the Faraday constant (96485 C mol^{-1}), I / µA is current, α is the transfer coefficient and n is the number of electrons participating in the rate control step that is considered to be 1. Using the Tafel slope, the value of α for carmoisine was found to be 0.56.

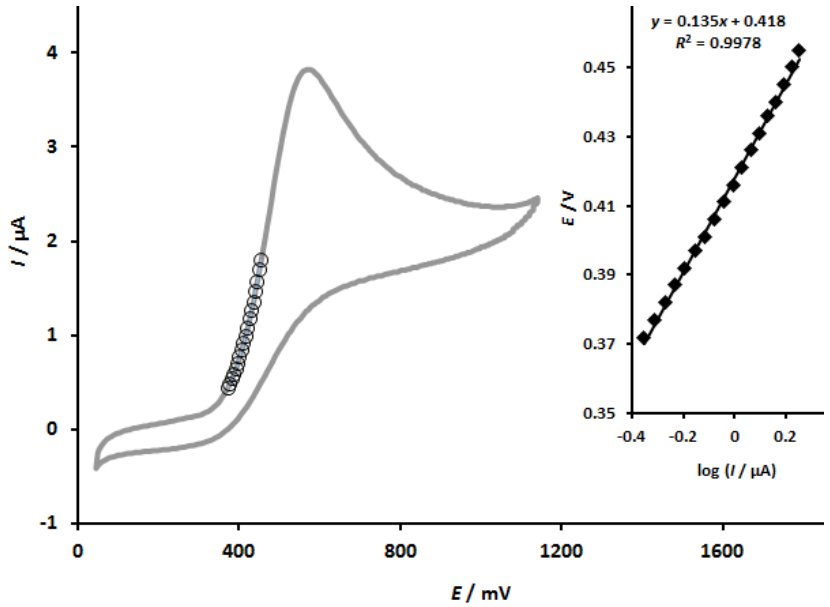

Figure 4. *CV captured for GO/NiO/CPE in phosphate buffer (0.1 M, pH 7.0) with carmoisine (100.0 µM) at the scan rate of 10 mV s^{-1}. Inset: Tafel plot derived from CV*

Chronoamperometry

We were able to calculate the diffusion coefficient for carmoisine using chronoamperometry, as the scan-rate analysis confirmed that carmoisine oxidation on the modified electrode was diffusion-controlled. To record chronoamperograms, the potential was stepped to 490 mV (Figure 5).

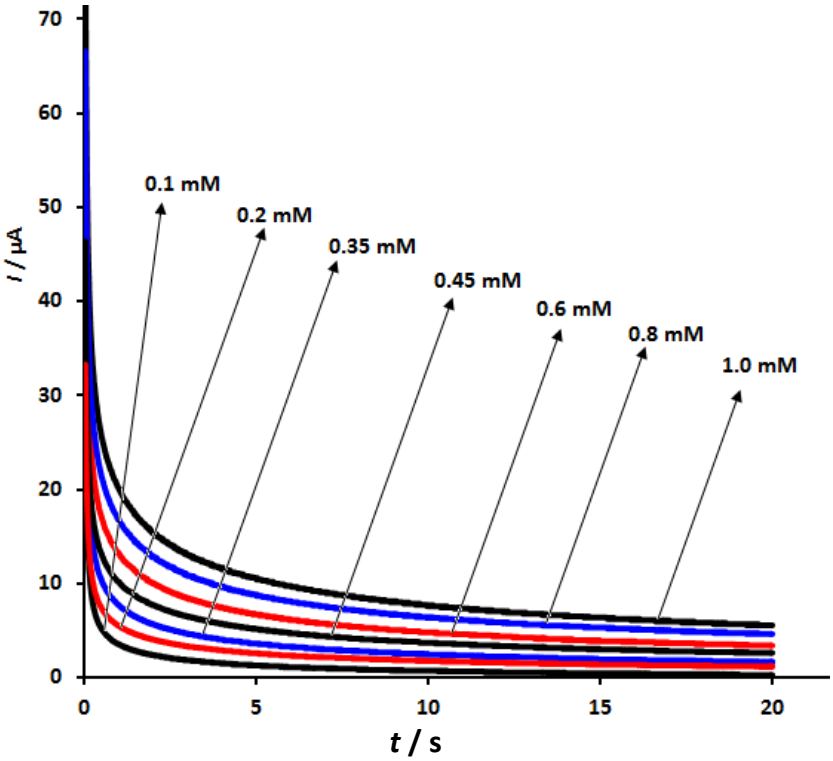

Figure 5. *Chronoamperograms for GO/NiO/CPE in phosphate buffer (0.1 M, pH 7.0) with different carmoisine concentrations (0.1 to 1.0 mM)*

A linear plot of *I vs.* $t^{-1/2}$ was constructed as the best fit for various carmoisine concentrations, as shown in Figure 6A. Figure 6B shows the slope plot of this straight line against carmoisine concentration. Using Cottrell's equation and plot slope, the mean diffusion coefficient for carmoisine was calculated to be 4.3×10^{-6} cm^2 s^{-1}.

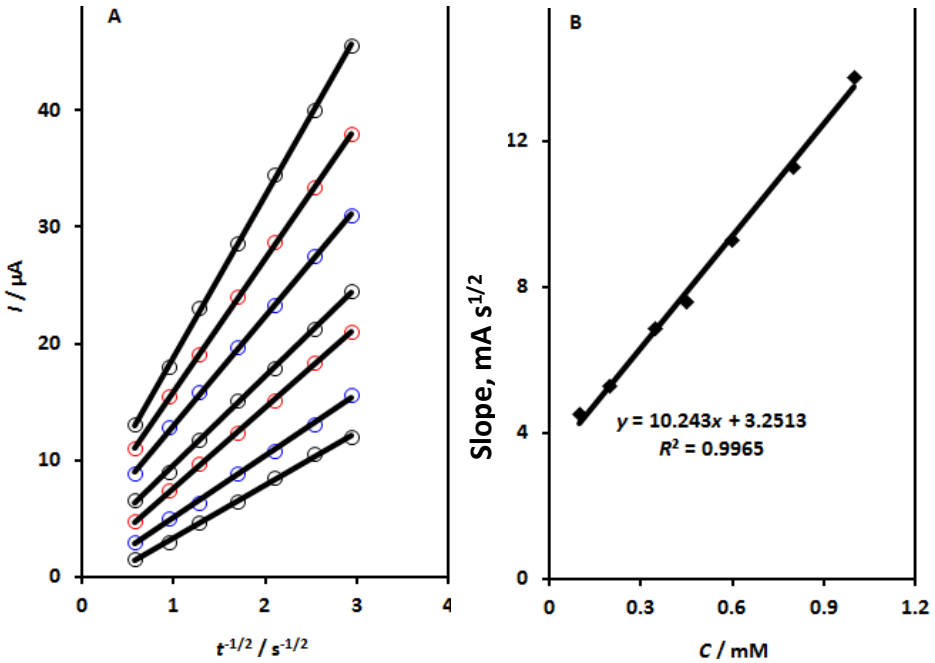

***Figure 6**. (A) Cottrell's plots for chronoamperograms in Figure 5, (B) slope diagram of straight lines versus carmoisine concentration*

Detection limit and standard curve

For the analytical determination of carmoisine, DPV was carried out for the modified electrode (Figure 7).

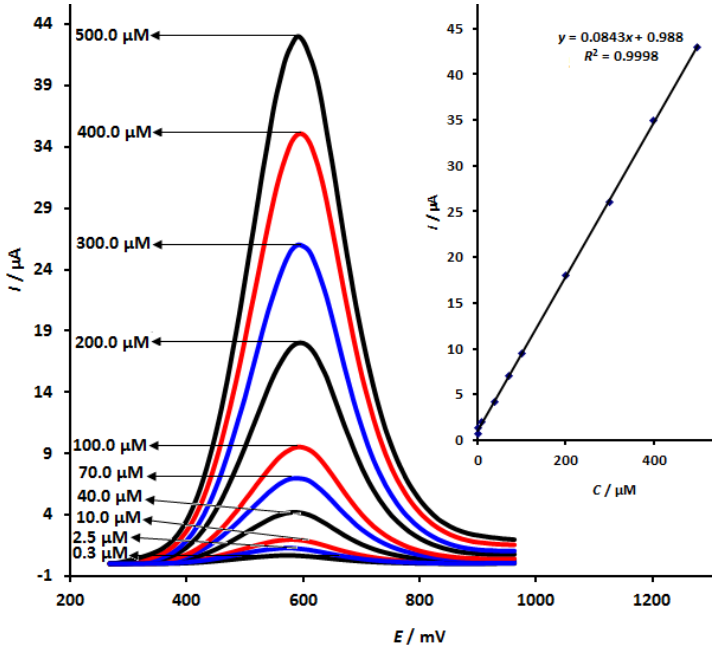

***Figure 7**. DPVs of GO/NiO/CPE in phosphate buffer (0.1 M, pH 7.0) with several carmoisine concentrations (0.3-500 µM). Inset: peak current as a function of carmoisine concentration*

In a 0.1 M phosphate buffer at pH 7.0, the distinctive peak current of carmoisine increased as the carmoisine concentration increased from 0.3 to 500.0 µM. Inset of Figure 7 displays the graph of the connection between peak rise and carmoisine concentration, indicating remarkable linearity with a linear dynamic range of 0.3 to 500.0 µM. The limit of detection (LOD) for the detection of carmoisine was found to be 0.1 µM.

Simultaneous differential pulse voltammetric analysis of carmoisine and tartrazine

Carmoisine and tartrazine were co-detected using the as-fabricated GO/NiO/CPE by simultaneously changing their concentrations. Figure 8 shows DPVs obtained for various concentrations of tartrazine and carmoisine at GO/NiO/CPE in 0.1 M phosphate buffer, pH 7.0. The recorded voltammograms show–that the anodic peaks at 590 mV and 1010 mV correspond to carmoisine and, tartrazine, respectively, suggesting that these azo-dyes may be detected concurrently on the surface of GO/NiO/CPE.

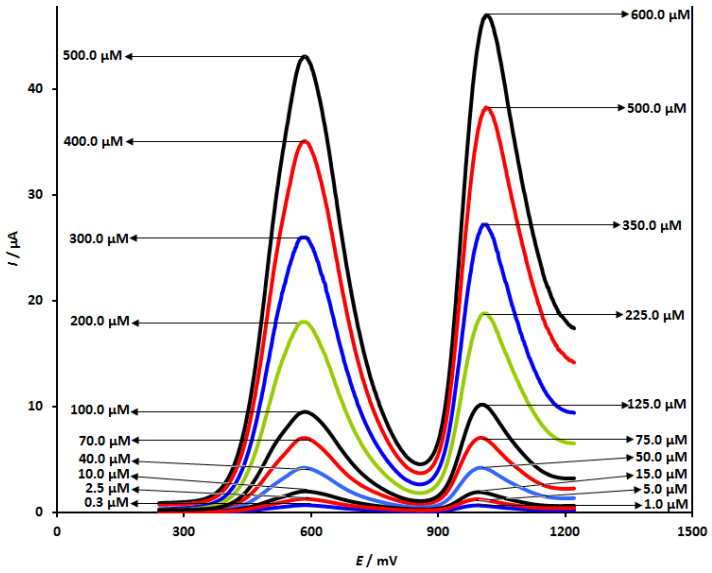

Figure 8. *DPVs for GO/NiO/CPE in phosphate buffer (0.1 M, pH 7.0) with different carmoisine and tartrazine concentrations*

The linearity of changes in the peak current of oxidation against varying concentrations of tartrazine and carmoisine is displayed in Figure 9.

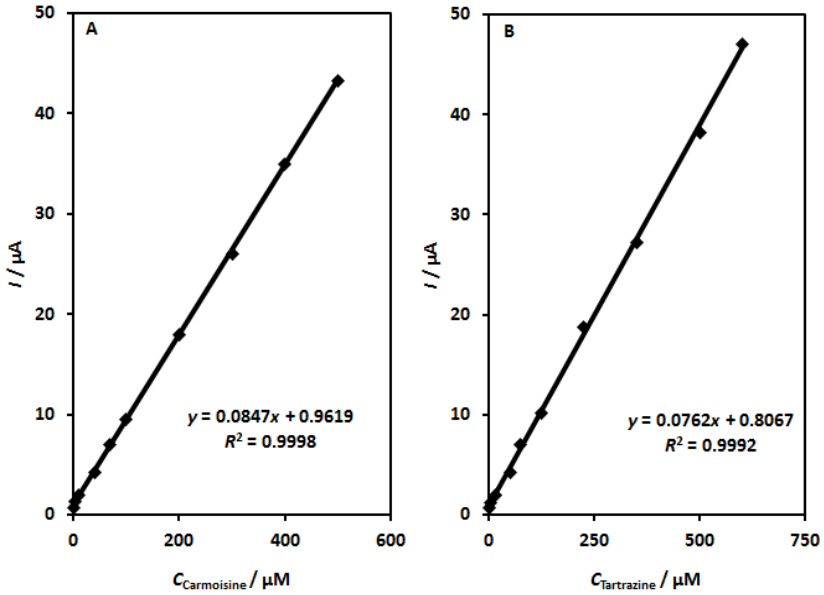

Figure 9. *I_{pa} vs. concentration of (A) carmoisine and (B) tartrazine for GO/NiO/CPE in phosphate buffer (0.1 M, pH 7.0). Data obtained from DPVs shown in Figure 8*

Repeatability, reproducibility, and stability

The DPV approach has been used to assess the repeatability, reproducibility, and stability of the GO/NiO/CPE. The 4.7 % relative standard deviation (RSD) for the same approach demonstrated the

exceptional repeatability of GO/NiO/CPE. The outstanding reproducibility of GO/NiO/CPE was demonstrated by an RSD of 3.5% across seven consecutive measurements of 100.0 µM carmoisine using the same electrode. The stability of GO/NiO/CPE was examined by keeping the modified electrode for a whole day. After 24 days, the oxidation current of carmoisine decreased to 96.9 % of its initial value, indicating that electrode storage was stable.

Interference studies

A GO/NiO/CPE sensor that detects 30.0 µM carmoisine in the presence of several species was investigated for interference. The concentration of interfering species that results in > ±5% change in the target analyte's peak current is considered the tolerance limit. The results showed that a 20-fold increase in glucose, alanine, tryptophan, and histidine, and a 50-fold increase in Na^+, K^+, Ca^{2+}, Mg^{2+}, NH_4^+, SO_4^{2-}, Cl^-, and Br^- concentration, do not interfere with the determination of carmoisine.

Analytical application of graphene oxide/NiO/carbon paste electrode

Using DPV to detect tartrazine and carmoisine in powdered juice specimens, the suitability of the as-fabricated electrode (GO/NiO/CPE) was examined. The findings are shown in Table 1. As can be observed, the computed recoveries had relative standard deviations (RSDs) ≤3.5 % and ranged from 97.7 to 103.7%. As a result, the GO/NiO/CPE's reaction was unaffected by the genuine specimens' matrix, indicating that it may be used for sensing in real specimens.

Table 1. *The analytical suitability of GO/NiO/CPE for detecting carmoisine and tartrazine in actual specimens, powdered juice (n = 5)*

Spiked concentration, µM		Found concentration, µM		Recovery, %		RSD. %	
Carmoisine	Tartrazine	Carmoisine	Tartrazine	Carmoisine	Tartrazine	Carmoisine	Tartrazine
0	0	2.9	3.4	-	-	3.5	3.0
2.0	2.0	4.8	5.6	98.0	103.7	1.9	2.6
4.0	4.0	7.0	7.2	101.4	97.3	2.6	2.8
6.0	6.0	8.7	9.5	97.7	101.1	2.9	1.8
8.0	8.0	11.3	11.2	103.7	98.2	3.1	2.1

Conclusions

This study effectively modified a CPE with a GO/NiO nanocomposite, enabling simultaneous electrochemical determination of tartrazine and carmoisine. The electrocatalytic performance of the developed GO/NiO/CPE sensing platform was greatly improved by the synergistic effect of GO and NiO. This sensor demonstrated its capacity for simultaneous determination in the samples by successfully differentiating the oxidation peaks of both substances. Additionally, the created sensing platform has notable benefits such as easy preparation, high sensitivity, and outstanding stability. Additional research is needed to assess the juice's performance and increase its usefulness.

Funding: *No funding for this work.*

References

[1] B. Peng, A. Jahanian, T.R. Collier, H. Peng, J.B. Behrendorff, R.E. Speight, Synthetic biology for sustainable food colourant production: Innovations and opportunities, *Food Chemistry* **503** (2026) 147749. https://doi.org/10.1016/j.foodchem.2025.147749

[2] F. Magesa, Y. Wu, Y. Tian, J.M. Vianney, J. Buza, Q. He, Y. Tan, Graphene and graphene like 2D graphitic carbon nitride: Electrochemical detection of food colorants and toxic substances in environment, *Trends in Environmental Analytical Chemistry* **23** (2019) e00064. https://doi.org/10.1016/j.teac.2019.e00064

[3] K. Damotharan, G. Sudhakaran, M. Ramu, M. Krishnan, J. Arockiaraj, Biochemical processes mediating neurotoxicity induced by synthetic food dyes: a review of current evidence, *Chemosphere* **364** (2024) 143295. https://doi.org/10.1016/j.chemosphere.2024.143295
[4] M. Kucharska, J. Grabka, A review of chromatographic methods for determination of synthetic food dyes, *Talanta* **80** (2010) 1045-1051. https://doi.org/10.1016/j.talanta.2009.09.032
[5] C. Illahi, W.E. Hutabarat, N. Nurdini, F. Failamani, G.T. Kadja, Photocatalytic degradation of azo dyes over MXene-based catalyst: recent developments and future prospects, *Next Nanotechnology* **6** (2024) 100055. https://doi.org/10.1016/j.nxnano.2024.100055
[6] M.L. Mello, E.H. Dos Anjos, B. de Campos Vidal, Usefulness of sulfonated azo dyes to evaluate macromolecularly oriented protein substrates, *Acta Histochemica* **126** (2024) 152154. https://doi.org/10.1016/j.acthis.2024.152154
[7] P. Srilaoong, J. Buasakun, C. Raksakoon, C. Sangma, K. Chainok, P. Harding, D. J. Harding, T. Duangthongyou, Highly effective detection of DNP and Fe^{3+} by designed coordination polymers containing electron rich linkers and azo functional groups, *Polyhedron* **233** (2023) 116300. https://doi.org/10.1016/j.poly.2023.116300
[8] F. Calogero, H. S. Freeman, J. F. Esancy, W. M. Whaley, B.J . Dabney, An approach to the design of non-mutagenic azo dyes: 2. Potential replacements for the benzidine moiety of some mutagenic azo dyestuffs, *Dyes and Pigments* **8** (1987) 431-447. https://doi.org/10.1016/0143-7208(87)85035-0
[9] T. Li, L. Wei, Y. Fang, Y. Cui, X. Wang, Y. Li, Risk identification of human health, ecotoxicity, and degradation products of azo dyes: development of a priority control list, *Environmental Pollution* **386** (2025) 127180. https://doi.org/10.1016/j.envpol.2025.127180
[10] F. Erek, A comparative study on magnetic solid phase extraction and magnetic colloidal gel based-dispersive solid phase extraction methods for preconcentration of carmoisine (E 122) in food samples, *Journal of Food Composition and Analysis* **139** (2025) 107091. https://doi.org/10.1016/j.jfca.2024.107091
[11] L. Micheletti, B. Coldibeli, C.A. Salamanca-Neto, L.C. Almeida, E.R. Sartori, Assessment of the use of boron-doped diamond electrode for highly sensitive voltammetric determination of the azo-dye carmoisine E−122 in food and environmental matrices, *Talanta* **220** (2020) 121417. https://doi.org/10.1016/j.talanta.2020.121417
[12] S. Datta, N. Mahapatra, M. Halder, pH-insensitive electrostatic interaction of carmoisine with two serum proteins: A possible caution on its uses in food and pharmaceutical industry, *Journal of Photochemistry and Photobiology B* **124** (2013) 50-62. https://doi.org/10.1016/j.jphotobiol.2013.04.004
[13] P. Amchova, F. Siska, J. Ruda-Kucerova, Safety of tartrazine in the food industry and potential protective factors, *Heliyon* **10** (2024) e38111. https://doi.org/10.1016/j.heliyon.2024.e38111
[14] S.S. Chaudhari, P.O. Patil, S.B. Bari, Z.G. Khan, A comprehensive exploration of tartrazine detection in food products: Leveraging fluorescence nanomaterials and electrochemical sensors: Recent progress and future trends, *Food Chemistry* **433** (2024) 137425. https://doi.org/10.1016/j.foodchem.2023.137425
[15] A. Dmukhailo, S. Tvorynska, L. Dubenska, Rapid and straightforward electrochemical approach for the determination of the toxic food azo dye tartrazine using sensors based on silver solid amalgam, *Journal of Electroanalytical Chemistry* **932** (2023) 117250. https://doi.org/10.1016/j.jelechem.2023.117250
[16] A. Obaid Imarah, N. Hasan, M.G. Alabbasi, ZnO-modified carbon paste electrode for electrochemical sensing of dopamine in the presence of tyrosine, *ADMET and DMPK* **13** (2025) 3010. https://doi.org/10.5599/admet.3010
[17] S. Bonyadi, K. Ghanbari, Application of molecularly imprinted polymer and ZnO nanoparticles as a novel electrochemical sensor for tartrazine determination, *Microchemical Journal* **187** (2023) 108398. https://doi.org/10.1016/j.microc.2023.108398

[18] R. Muslim Muhibes, F. A Khazaal, Q.M. Salih, R. Radi Karabat, Electrochemical determination of calcium folinate in the presence of methotrexate and 5-fluorouracil using UiO-66/CdS composite modified screen-printed carbon electrode, *ADMET and DMPK* **13** (2025) 2897. https://doi.org/10.5599/admet.2897

[19] P. Saini, R. Aggarwal, A. Joshi, S. Bansal, Fabrication of activated carbon electrodes for energy storage devices using waste biomass: A review, *Journal of Power Sources* **676** (2026) 239868. https://doi.org/10.1016/j.jpowsour.2026.239868

[20] S. Mir, N. Akbarzadeh Torbati, V. Amani, S. Tajik, H. Beitollahi, Y-Co metal-organic framework for sensitive electrochemical determination of doxorubicin hydrochloride, *ADMET and DMPK* **13** (2025) 3141. https://doi.org/10.5599/admet.3141

[21] M. Achache, S. El Boumlasy, D. Bouchta, M. Choukairi, Development and applications of carbon paste and Sonogel-Carbon electrodes modified with nanomaterials: Perspectives in pharmaceutical, biological, environmental and food analysis: A review, *TrAC Trends in Analytical Chemistry* **194(A)** (2025) 118502. https://doi.org/10.1016/j.trac.2025.118502

[22] M. Mekersi, M. Ferkhi, A. Khaled, N. Maouche, M. Foudia, E.K. Savan, Electrochemical bio-monitoring of the analgesic drug paracetamol, the antipsychotic sulpiride, and the antibiotic bromhexine hydrochloride using modified carbon paste electrode based on $Ca_{0.7}La_{0.3}Fe_{0.3}Ni_{0.7}O_3$ nano-sized particles and black carbon, *Surfaces and Interfaces* **53** (2024) 104941. https://doi.org/10.1016/j.surfin.2024.104941

[23] M.R. Baezzat, Z. Pourghobadi, R. Pourghobadi, Nanomolar determination of Penicillin G potassium (PGK) salt using a Carbon Paste Electrode modified with TiO_2 nano particles/Ionic Liquids in real samples, *Materials Chemistry and Physics* **270** (2021) 124641. https://doi.org/10.1016/j.matchemphys.2021.124641

[24] C.V. Gopi, S. Alzahmi, M.Y. Al-Haik, Y.A. Kumar, F. Hamed, Y. Haik, I.M. Obaidat, Recent advances in pseudocapacitive electrode materials for high energy density aqueous supercapacitors: Combining transition metal oxides with carbon nanomaterials, *Materials Today Sustainability* **28** (2024) 100981. https://doi.org/10.1016/j.mtsust.2024.100981

[25] S. Santangelo, F. Pantò, C. Triolo, S. Stelitano, P. Frontera, F. Fernández-Carretero, I. Rincon, P. Azpiroz, A. García-Luis, Y. Belaustegui, Evaluation of the electrochemical performance of electrospun transition metal oxide-based electrode nanomaterials for water CDI applications, *Electrochimica Acta* **309** (2019) 125-139. https://doi.org/10.1016/j.electacta.2019.04.075

[26] R. Singh, A. Singh, A. Dubey, A. Ahmed, A.K. Sundramoorthy, S. Arya, Synthesis and characterization of spherical NiO nanoparticles as a high-performance supercapacitor electrode, *Next Research* **4** (2025) 101226. https://doi.org/10.1016/j.nexres.2025.101226

[27] L. Zhao, A. Piper, G. Rosati, A. Merkoçi, Direct writing of graphene electrodes for point-of-care electrochemical sensing applications, *Sensors & Diagnostics* **3** (2024) 1406-1427. https://doi.org/10.1039/d4sd00140k

[28] S.A. Zaidi, Graphene: a comprehensive review on its utilization in carbon paste electrodes for improved sensor performances, *International Journal of Electrochemical Science* **8** (2013) 11337-11355. https://doi.org/10.1016/S1452-3981(23)13189-0

A.S. Khodkina, M.A. Ovchinnikov, I.E. Rasskazov, A.V. Kolchin, D.V. Korolev, E.I. Kunitsyna, M.V. Bakhmetiev, S.I. Serebrennikova, V. Ibragimova, N.D. Mitiushev, E.N. Kabachkov, Synthesis of hybrid materials based on reduced graphene oxide and Ni (NiO) nanoparticles by supercritical solvent and thermal treatment techniques, *Materials Science and Engineering B* **324** (2026) 118950. https://doi.org/10.1016/j.mseb.2025.118950